THERESA GARLEY
TECHNICAL LIBRARY
DOCUMENT DELIVERY
SANDIA NATIONAL LABORATORIES
PO BOX 5820
ALBUQUERQUE, NM 87185-5820
UNITED STATES

ORDER NUMBER:	**CI-04852031-6**
Account Number:	FGH58514
Delivery Mode:	ARI
Delivery Address:	132.175.164.7
Submitted:	2004/08/04 10:37:30
Received:	2004/08/04 10:37:30
Printed:	2004/08/04 12:44:03

Direct **Periodical** **WWW Catalogue** **UNITED STATES**

Client Number:	NELSON BELL
Title:	**JOURNAL OF NANOSCIENCE AND NANOTECHNOLOGY**
DB Ref. No.:	IRN19462451
ISSN:	15334880
Vol./Issue:	VOL 4/ NO. 3
Date:	2004
Pages:	283-
Article Title:	DISPERSION PROPERTIES OF AN ALUMINA NANOPOWDER....
Article Author:	BELL
Report Number:	IRN19462451
Publisher:	AMERICAN SCIENTIFIC PUBLISHERS,
Information Source:	INNOPAC

INSTRUCTIONS: 1846/ 1411

Estimated cost for this 8 page document: $10.8 document supply fee + $0 copyright = $10.8

Dispersion Properties of an Alumina Nanopowder Using Molecular, Polyelectrolyte, and Steric Stabilization

Nelson S. Bell* and Mark A. Rodriguez

Sandia National Laboratories, Albuquerque, New Mexico, USA

A commercial alumina nanopowder was characterized and its dispersion was studied using electrostatic, electrosteric, and steric surfactants. Citric acid was used as the electrostatic dispersant, ammonium polymethacrylic acid (Darvan C) as the electrosteric dispersant, and Hypermer KD-1 in α-terpineol as a purely steric system. Phase stability in water was examined by X-ray diffraction, and the surface chemistry was characterized by zeta potential and isoelectric points. Rheology measurements were used to study the impact of each dispersant type on maximum solids loading, with the maximum loading being achieved for the polyelectrolyte dispersant. Differences in maximum solids loading are related to the excluded volume of the particle separation distance induced by each stabilizing interaction.

Keywords: Nanoparticle, Dispersion, Alumina, Rheology, Acoustic Spectrometry.

1. INTRODUCTION

Nanomaterials raise a number of possibilities for improvement of material properties. Examples of the exploitation of nanomaterial properties include development of ultrafine grain size products or nanostructured composites.[1] In addition, nanoparticles are also used to lower the reaction temperature or conversion rate of bulk materials.[2–4] The production of nanoparticles has great potential to impact processing science, but use of these materials raises a number of questions beyond traditional powder processing technology because of their small size. These questions include the formation of hard (i.e., sintered) aggregates during synthesis or processing, phase stability of the nanosized materials, variation in surface chemistry, and dispersion forces between nanoparticles. When dispersion of nanoparticles is considered, a robust dispersion mechanism is increasingly important, because the number concentration of a nanosized dispersion is much higher than that with conventional powders, and the frequency of potential aggregation events is increased.

With conventional powder processing methods, the achievement of maximum solids loading in a suspension directly relates to improvements in final performance by reducing flaw size and concentration, increasing grain size uniformity, and reducing shrinkage, stress, and other benefits. The solids loading of conventional powders can be as high as 60 vol % or greater for the proper mixtures of particle sizes. In these systems, the length of the interaction used to stabilize the suspension is nearly negligible compared with particle diameters; however, with nanoparticles, the same stabilizing interactions are a significant fraction of the particle diameter and begin to have a deleterious effect on the achievable solids content of a fluid dispersion. These effects are generally related by the following equation for monosized particles:

$$\phi_{\text{eff}} = \phi\left(1+\frac{\delta}{r}\right)^3 \tag{1}$$

Here δ is the thickness of the dispersant interaction length, and r is the radius of the particle. The effective packing fraction ϕ_{eff} is often taken as that of randomly packed uniform spheres (0.63) but can vary based on particle size distribution, and ϕ is the true volume fraction of the powder. The effective volume fraction is always higher than the true volume fraction. This relationship sets a boundary for discussion of what constitutes a nanosized powder. From colloidal probe measurements of a number of typical commercial surfactants, the separation distances generated are on the order of 5–15 nm.[5–8] Figure 1 shows that for particle sizes below 100 nm, the separation distance generated by the dispersant begins to affect the maximum attainable solids loading. The severity of the phenomenon increases as the particle size is lowered and as the steric length increases. In a previous study in 6 nm titania suspensions it was stated that only polyacrylamide of molecular weight near 100,000 was sufficient to stabilize the particles against aggregation by providing a steric layer

*Author to whom correspondence should be addressed.

  1533-4880/2004/04/283/554/$17.00+.25 doi:10.1166/jnn.2004.027

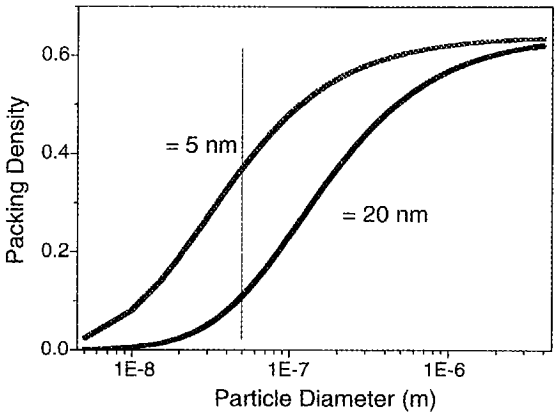

Fig. 1. True solids loading curves for nanopowder suspensions with particle steric barriers of 5 and 20 nm. The maximum packing fraction is taken to be the same as random monodisperse sphere packing. The vertical line indicates the disparity between true volume fractions for a 50-nm-diameter particle suspension.

thickness of 6 nm.[9] This steric length is equal to the particle diameter and limits the applications of these kinds of nanoparticle dispersions.

Dispersant molecules can be characterized by the forces they generate, which counter the attractive van der Waals interaction. Small molecule dispersants are low molecular weight additives that specifically adsorb to the surface and often generate a strong surface charge. Lipids fall into this category as well as multicharged acids that chemically complex with the surface. Their small size generally prevents the formation of a significant steric barrier to agglomeration, so their stabilization mechanism is largely electrostatic. Electrostatic stabilization is also possible on the native particle surface under the proper conditions of pH if there are enough ionizable surface groups. Electrostatic methods will be increasingly defeated at high salt concentrations due to screening effects and counterion condensation at the interface. Steric stabilization is generated by the adsorption of uncharged polymers that have extended loops and tails. When particles are in close proximity, there are entropic and osmotic repulsions generated between the particle surfaces. Polyelectrolytes are also commonly used as dispersants that combine both the electrostatic repulsion and steric interactions between surfaces. Polyelectrolytes have been reported to act as efficient dispersants for 20-nm ceria particles.[10]

In this study, we analyzed the impact of these three classes of dispersants on a newly available nanosized alumina powder. The powder was characterized for its morphology, phase stability, and dispersability. The rheology of the powder was examined in its native state as well as with a small molecule electrostatic dispersant, a linear polyelectrolyte, and a nonaqueous, steric copolymer. Both the rheological profile versus shear rate and the rise in viscosity with solids loading were examined to describe the effectiveness and processing range of these dispersants. Conclusions are drawn about the potential for using nanoparticle materials in conventional processing methods and about the type of molecules needed to promote the most effective dispersion of nanosized powders.

2. EXPERIMENTAL DETAILS

The alumina powder was generously donated by TAL Materials. It is produced by liquid-feed flame spray pyrolysis of metalloorganic $[N(CH_2CH_2O)_3N]$ alumatrane by a vapor phase condensation method.[11] It is composed of a mixture of transition alumina phases, primarily δ. The density of the powder was measured using a helium pycnometer and found to be 3.5 g/cm^3.

The powder surface area was measured using an accelerated surface area and porosimetry system (ASAP) 2010 by Micromeritics. The sample was degassed at 350°C for 12 h to remove adsorbed water and CO_2. The surface area is 42.20 ± 0.07 m^2/g. Transmission electron microscopy was performed on the as-received powder dried on a carbon grid from aqueous suspension. The transmission electron microscope was a Phillips CM30 operating at 300 kV.

X-ray diffraction was performed using a Siemens D500 powder diffractometer equipped with a Cu sealed tube source and a diffracted beam graphite monochromator. A 1° silt size was used for divergence, scatter, and receiving slits. Diffraction scans were collected from 10–80° 2θ using a step-size of 0.05° and a 4-second count time. The powder phase stability in aqueous suspension was studied by aging in aqueous suspension at pH 9 and characterizing the recovered powder.

Characterization of the particle size distribution in suspension and zeta potential was performed using a DT 1200 acoustic spectrometer (Dispersion Technology, Mount Kisko, NY). The operational details of the instrument are described in Refs. 12 and 13. Samples were prepared at 1 vol % in water and dispersed using an ultrasonic horn programmed to emit 15 W in 1-s intervals for a duration of 6 min. Dispersant additions for the aqueous samples were made before sonication, and any pH adjustment was performed after sonication.

Rheological measurements were performed on a Haake RS300 rheometer using a cone and plate configuration with 1° cone angle and 60-mm diameter. The plate temperature was maintained at 25°C by a recirculating fluid pump. Rheological characterization was performed using a 120-s preshear at 400 s^{-1} with 1 min of no motion, followed by a shear rate ramp from 0.1 to 400 s^{-1} over 120 s, a hold at 400 s^{-1} for 30 s, and then a decrease in the shear rate back to 0.1 s^{-1} over 120 s. Samples for testing were made by adding dispersants to solvent in the proper proportion to form a 30 vol % suspension, and powder was added and mixed using an ultrasonic horn as needed to generate a fluid dispersion. For suspensions that did not

flow under gravity, an ultrasonic bath was used to remove air bubbles from the suspension and prepare samples for rheological characterization. Successive measurements in the rheometer were performed by diluting the sample with pure solvent and remixing using the ultrasonic horn for the initial samples and the ultrasonic bath once viscosity became low and the sample exhibited fluid behavior. For the determination of relative viscosity, the solvent viscosity of α-terpineol was measured from 200 to 2000 s^{-1} and gave an average value of 29.4776 mPa.

3. RESULTS

Figure 2 shows the powder morphology via transmission electron microscopy. The micrographs indicate that the powder is composed of primarily spherical or equiaxed particles that appear to be single crystals. The variance in particle size is between approximately 10 and 400 nm. The sizes of some of the particles are greater than 100 nm, but a majority of particles are less than 100 nm in size. Most striking about this powder is the absence of any discernible agglomerates. A number of micrographs were examined, and no agglomerates were visible in any of the photos. This result is remarkable in that hard (i.e. sintered) agglomeration is typical of a number of nanopowders produced via vapor phase decomposition. Hard agglomerate formation is often a critical concern in forming a dispersion of low viscosity.

Figure 3 shows x-ray diffraction data taken from native powder and after weeks of aging at pH 9. The as-received sample showed the presence of at least three phases: θ-alumina (PDF 86-1410), δ(tet)-alumina (PDF 46-1131), and δ(ort)-alumina PDF (46-1215). It does not indicate any of the gamma phase identified in powders described in prior publications.[11] For the aged samples, an additional minor phase of bayerite (PDF 83-2256) was also observed as indicated by the asterisks in Figure 2 (inset). Using the diffraction data in the 18–22° 2θ range, we were able to estimate the phase fraction of bayerite. By using reference intensity-ratios[14] from the PDF cards and quantified data from a prior publication[11] and by assuming that the peak at ~19.5° 2θ is due entirely to the θ-alumina phase, phase fractions for the bayerite were determined to be approximately 1–2 wt % for the three aged samples.

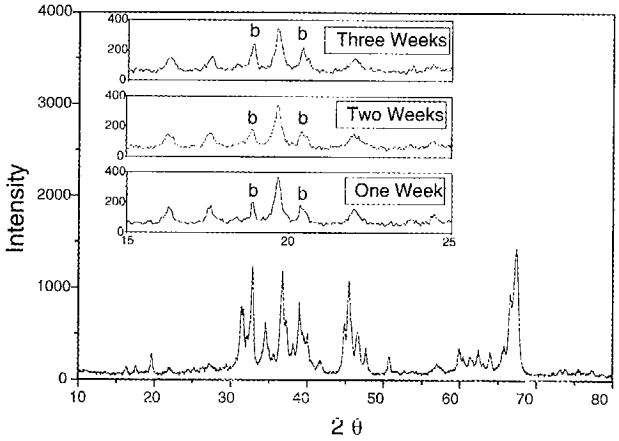

Fig. 3. Phase composition of the powder as a function of aging time in aqueous suspension. The insets show the increase in bayerite peaks after aging at pH 9.

Figure 4 presents the zeta potential data collected for the native powder, powder dispersed with Darvan C, and several dispersions with varying levels of citric acid additions. The isoelectric point can be adjusted easily by using citric acid. The concentration of Darvan C used in this pH titration was chosen by monitoring the zeta potential of the

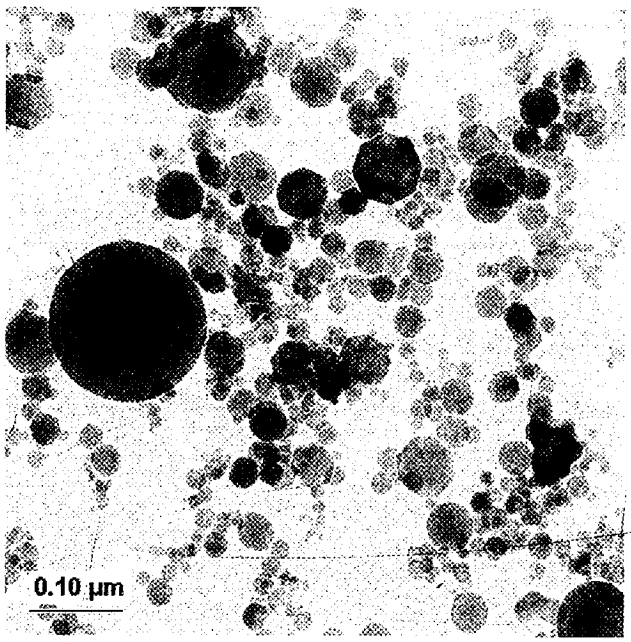

Fig. 2. Transmission electron micrograph of the as-received alumina powder.

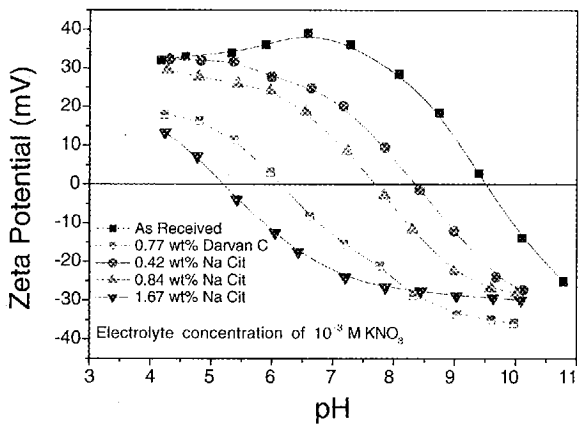

Fig. 4. Zeta potential characterization of the powder as received, with Darvan C dispersant, and varying concentrations of citric acid (Na Cit).

RESEARCH ARTICLE

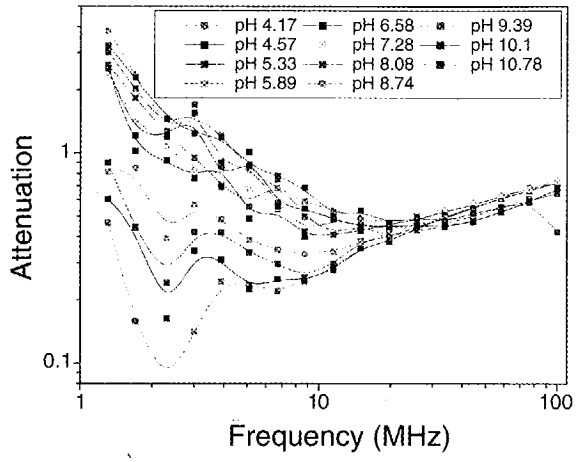

Fig. 5. Acoustic attenuation spectra versus frequency for the as-received TAL alumina powder as a function of pH.

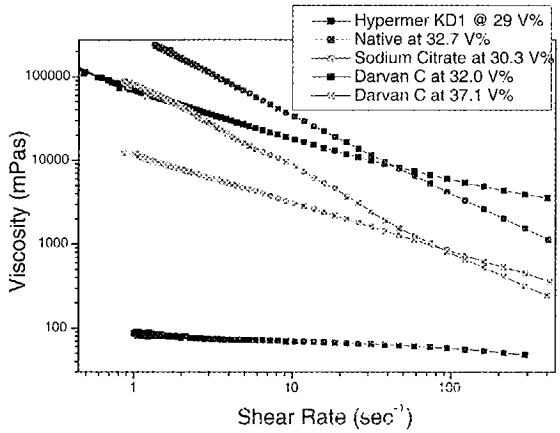

Fig. 6. Rheological comparison of the TAL alumina powder dispersed with each dispersant near the solids content of 30 vol %. The Darvan C dispersed sample is also presented at 37.1 vol % to show its behavior at viscosity similar to that of the other samples.

native powder at pH 9 as the dispersant was titrated into the suspension, and surface coverage was assumed to be complete when the zeta potential remained constant against additional titration (not shown). The isoelectric point for this concentration of Darvan C is approximately 6 and produced the highest values of zeta potential at pH 9, at which both citric acid and the Darvan C dispersant are expected to be fully deprotonated and generate the maximum negative zeta potential. The zeta potential values had a magnitude of less than −40 mV for any dispersant addition or pH condition.

Figure 5 shows the acoustic spectra of the native powder as measured for each pH during the titration from pH 4 to pH 11. These scans show excellent uniformity of the data points at frequencies greater than 20 MHz, but at lower frequencies, there is a progressive increase in attenuation as pH increases until a rough equilibrium is established above pH 6.58. Table I presents the particle distribution estimates determined from the acoustic spectroscopy data during the titration using data between 8 and 100 MHz and indicates that the mean particle size begins to increase near pH 6.58.

Table I. Fitting parameters and particle size predictions of the native TAL alumina powder in 10^{-3} M KNO_3 solution versus pH titration.

pH	Zeta potential	Structure factor	Mean size (nm)	Standard deviation (nm)	% error
4.17	32.07	0.9	52.7	497	2.3
4.57	33.03	0.9	53.9	590	2.9
5.33	34.03	0.9	54.6	572	2.7
5.89	36.09	1.0	56.3	657	1.3
6.58	39.06	1.1	80.7	870	1.5
7.28	36.12	1.0	111	860	4.1
8.08	28.54	0.1	411	830	3.7
8.74	18.5	0.2	687	690	7.1
9.39	2.87	0.1	564	890	7.0
10.1	−13.82	0.1	615	780	6.4
10.78	−25.07	0.1	543	680	6.7

The "% error" column refers to the error between the measured data and the calculated values of the attenuation spectra. The structure factor characterizes particle association without aggregation, and it is described further in the "Discussion." The inclusion of data points below 8 MHz created very high error values, and the zeta potential values calculated for the system differed by less than 2 mV by exclusion of the low-frequency data. The change in attenuation spectra and development of aggregates correlate for a number of systems.[12]

Figure 6 shows the rheology characterization determined for each dispersant near a solids loading of 30 vol %. The rheology of the Darvan C dispersed suspension at approximately 37 vol % is also presented to show the profile near its maximum in solids loading. The native powder was characterized at pH 5.4, the sodium citrate and Darvan C additions were both performed at pH 9, and the Hypermer KD1 was added in α-terpineol solvent. The added amount of Darvan C was found qualitatively to be higher than that determined from zeta potential measurements. The value chosen for rheology characterization was determined via measurements of viscosity at 15 vol % solids as a function of added dispersant. Figure 7 compares the reduced viscosity of each dispersant versus volume fraction and the fit of the modified Krieger–Doughtery equation, given in Table II.

4. DISCUSSION

The equilibrium phase of alumina at room temperature and pressure is gibbsite, but bayerite is also stable. In processing these powders, it is possible to observe a phase transformation of the surface to an alumina hydroxide chemistry.[15] In addition, nanopowders are known to be more soluble than conventional powders because of their high

RESEARCH ARTICLE

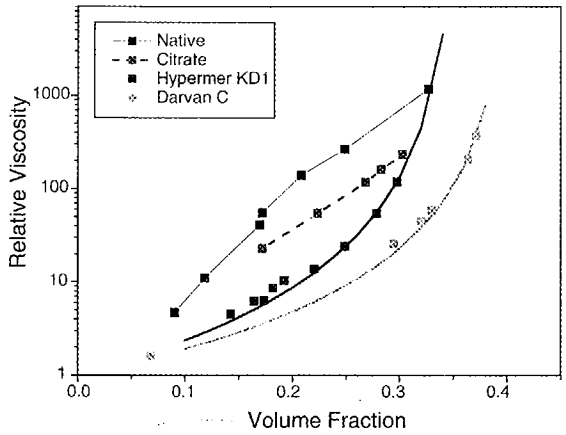

Fig. 7. Relative viscosity versus volume fraction for each dispersant at optimum concentration at a shear rate of 400 s^{-1}. Lines are drawn to guide the eye for the native and sodium citrate dispersed powders. The solid lines for the Hypermer KD1 and Darvan C dispersions are the Krieger–Doughtery equation fits with parameters given in Table 2.

surface curvature as related by the Ostwald-Freundlich equation:

$$S_r = S_0 \exp\left[\frac{2\gamma_{sl}V_m}{RTr}\right] \quad (2)$$

Here S_0 is the solubility of a flat surface, V_m is the molar volume of the material, γ_{sl} is the interfacial free energy, R is the gas constant, T is absolute temperature, and r is the radius of the particle. The potential for increased solubility or variation in phase was shown to affect future processing of nanopowders by Kwon and Messing,[16] who found that the formation of hard agglomerates relates to the dissolution and reprecipitation of solute at particle contacts during drying. In Figure 2, the phase stability of the powder is slightly unstable with respect to the formation of a small amount of bayerite phase. Because the crystalline phase was detected, it is unlikely that a purely surface phase reaction has occurred in the powder. More likely, the smallest particles have undergone either dissolution and reprecipitation or an *in situ* phase transformation to bayerite. Bayerite is typically produced by the slow carbonation of sodium aluminate solutions at 30–35°C, but there are a number of methods based on the reaction of an aluminum source with water as long as the source is of very fine size.[15, 17] The solution pH for the aging study was pH 9, at which the transition from the neutral $Al(OH)_3(aq)$ ion to the $Al(OH)_4^-$ anion is occurring. It is likely that at more alkaline pH the formation of an aluminum hydroxide precipitate will be promoted by the increased dissolution rate of the smallest nanoparticles. For this study, the bayerite quantity is not very significant, and the overall phase stability of the powder can be considered to be quite good.

Table II. Krieger–Doughtery function parameters for dispersed suspensions.

Dispersant	Maximum packing fraction, ϕ_{max}	Viscosity exponent, n
Darvan C	40.171%	5.69
Hypermer KD-1	35.385	7.36

The dispersion of conventional powders and their rheological properties relate rather closely to the calculated profiles of the DLVO theory.[8] All identical materials exhibit an attractive interaction due to dipole interactions between molecules, which are collectively considered as van der Waals forces and characterized by the material Hamaker constant.[18] As determined by X-ray diffraction measurements, this powder is a mixture of phases that should be expected to have slightly differing van der Waals interactions. The particle size also impacts the strength of the interaction and thereby its interparticle stability range. For steric surfactants, either theories of the compression of adsorbed polymer layers are used to counteract the attractive van der Waals interaction or a hard separation distance is chosen based on a estimate of the adsorbed layer thickness.[19] In the case of electrostatic repulsion, the value of the zeta potential is often chosen as the surface potential for calculations of interparticle forces. These forces are also impacted by the solution electrolyte concentration, known to reduce the range of repulsion as ionic strength increases. Rowlands et al.[20] showed that at extremely high salt concentrations (3 M) the background cations adsorb on the surface of the particles to affect their zeta potential.

When dispersion of nanoparticles is examined, a number of factors in the typical consideration of the optimum method for dispersion change. The powder surface area is increased and thereby the demand for a dispersant increases. In addition, the effects of curvature on the adsorbed amount and the interaction energy between particles are relatively unknown. For ionic dispersants, the higher dispersant concentration will introduce elevated concentrations of background electrolytes and collapse the repulsive forces between particles, especially as solids loading is maximized. Predictions of the interactions between nanoparticles by Kallay and Zalac[21] suggest that electrostatic repulsion will fail for nanoparticles and that nanoparticles will aggregate more rapidly than micron-sized particles due to their higher number concentration.

In this study, we compared the effectiveness of conventional surfactants in the dispersion of a powder in which the main particle size is small enough that the interaction length of the stabilizing interaction significantly impacts the maximum solids loading achievable in the system as well as the rheological characteristics. For that reason, the evaluated surfactants were chosen as a small molecule surfactant that is expected to have an extremely small steric component, a linear polyelectrolyte, and a purely steric polymer. In this study, the differences in molecular weight

that affect polymer interactions were not able to be characterized, but the products used are all commercially available and have a history of use in industrial processes.

The stability of a suspension can be evaluated from the acoustic attenuation spectra taken by our instrument and presented in Figure 5. Under acidic pH, the acoustic attenuation spectra versus frequency provides low adsorption that is similar to published values for the nanosized Ludox standard used to calibrate the instrument.[12] Table I presents the particle size distribution data for the native powder as a function of the pH titration. Aggregation occurs at and above pH 6.58 as shown by the increase in the mean particle size.

There are six loss mechanisms in acoustic spectroscopy: (1) viscous losses, (2) thermal losses, (3) scattering losses, (4) intrinsic losses, (5) electrokinetic losses, and (6) structural losses. Usually only the first four are treated, but structural losses can be significant. For dense rigid submicron particles at 1 to 100 MHz frequencies, the viscous losses are dominant. They are due to the shear wave generated by the particle oscillating in the acoustic pressure field. However, the theoretical treatment used by the instrument has another fitting component called the structure factor. The structure factor is a fitting parameter treating those losses in the system that relate to the forces between particles. The theoretical treatment models these forces as flexible "strings" connecting particles. This factor is initially large in the region of nanoparticle stability and decreases to a small value during the aggregation process. The acoustic data indicate that in the region of nanoparticle stability, there are forces between the particles that cause their association. Velegol et al.[22] showed that in systems in which the particle zeta potential is nonuniform, tangential forces can be developed between particles that cause a nontouching association. For this multiphase alumina powder, it is possible that the slight variations in van der Waals attraction and surface potential between the various phases and sizes are forming these nontouching particle associations. Once aggregation has occurred, these forces are no longer present between the large particle aggregates formed in the system. The process is more interesting in that this structure factor parameter actually appears to attain a maximum immediately before the system instability. Considering the balance of attractive van der Waals and stabilizing electrostatic forces in the system, the loss of strength of the stabilizing force as surface charge decreases would lead to a deeper secondary minimum in the interaction profile between particles until aggregation events are strong enough to lead to irreversible aggregation in the primary minimum. The prior work testing the use of the structure factor suggested that it would become significant under conditions of high solids loading approaching 40 vol %.[12] The additional insight into these nanoparticle suspensions is a surprising result.

Previously, citric acid (and its variant salts) and other molecular dispersants were studied with several alumina powders.[23–28] The citrate ion adsorbs to alumina surfaces by a ligand exchange process to form surface groups. Two of the three carboxylic acid groups and the hydroxyl group interact as part of the surface complex, and the third carboxylic acid group is directed toward the solvent. When deprotonated, it generates high absolute values for the surface potential. The adsorbed amount of citrate ions is pH dependent. Hidber and Gauckler[25] showed that for a powder with surface area of 10 m^2/g, complete adsorption occurred for concentrations under 0.2 wt % in the pH range of 3 to 7. The isoelectric point could be shifted to 3.4 from 9.1 by the addition of 0.4 wt % citrate. When adjusted for the surface area of the TAL powder, the amount of sodium citrate needed to achieve the same effects is higher. The equivalent ratio of citrate wt % of 1.7 should shift the isoelectric potential to 3.4, but only produces a value of 5.3. The high surface area of the powder provides a greater number of surface charge groups than conventional alumina powder. The higher ionic strength necessary to maintain electroneutrality will screen the electrostatic repulsion between charged surface groups and allow for increased citrate ion adsorption. Therefore, this powder may have a slightly higher adsorption capacity than a conventional alumina. Also, if there is increased dissolution of the powder, some citrate will form chelate complexes in solution rather than a surface complex.

Within the effects postulated, the behavior of citrate ion as a dispersant is similar to that found in prior investigations. However, the comparison between zeta potential values shows greater differences. Our measurements of zeta potential appear to maximize at −32 mV. Hidber et al.[26] found zeta potential values of approximately −65 mV under similar conditions. In contrast, Dietrich et al.[10] measured values for 20-nm ceria particles and found zeta potential values lower than −40 mV both on the native powder and with the use of polyelectrolyte dispersants, but their ionic strengths were not specified. All three measurements were performed using electroacoustic methods with calibration standards. Hidber and Gauckler[25] studied 500-nm particles, and the larger particle size may be the difference between the values. The low values determined for the nanosized materials raises a potential concern for nanoparticle processing, as loss of electrostatic stability at short range will lead to irreversible aggregation. Estimates of conditions required for nanoparticle stability suggest that electrolyte concentration should be less than 10^{-4} M, and the particle zeta potential should be high (40–50 mV).[29] Ionic strengths of 10^{-3} M or higher were shown to lower the zeta potential value significantly. The amount of dispersant, acid or base and the associated counterions increase in concentration as the amount of water decreases. The result is that at high solids concentration, the background electrolyte concentration can be as high as 1 M. Therefore, it is very important to know whether high zeta potential values can be generated under elevated electrolyte levels. The lower values of zeta potential measured here suggest

that the powder will not generate strong electrostatic surface interactions.

For a molecular dispersant such as sodium citrate, the steric interaction of the particle is very short range and most of the effectiveness of the molecule is due to the generation of a high zeta potential under alkaline pH conditions. To add the additional steric component to the powder stabilization, polyelectrolytes are commonly used to disperse ceramic powders.[30, 31] For polyelectrolyte surfactants such as Darvan C [which is poly(methacrylic acid)], there is both an electrostatic component to repulsion due to the carboxylic acid groups in the polymer and a steric repulsion resulting from the polymer conformation. The polymer conformation is a sensitive function of the salt concentration, pH, adsorbed amount, and system history. Studies of similar surfactants such as poly(acrylic acid) show that increasing salt concentrations lower the extension of the polymer from the surface due to screening of electrostatic repulsions between ionized groups on the polymer chain.[5–8]

The amount of dispersant needed to form a stable suspension was first considered using a titration of a suspension with the dispersant at pH 9 until a constant zeta potential value was obtained, and the mass of dispersant to the powder was found to be 0.77%. Additional surfactant did not raise the value of the zeta potential, and the titration of this concentration is shown in Figure 4. When suspensions of higher concentration were prepared, it was obvious that the powder was not dispersed. Rheology measurements at 15 vol % TAL alumina were performed to determine the point of minimum viscosity with added surfactant. The dispersant concentration that stabilized the suspension was found in this manner to be 3.16 wt % polymer. Conventional powders have required as little as 0.2 wt % polyelectrolyte to achieve 60 vol % fluid suspensions.[32] Clearly the additional surfactant needed to disperse a concentrated suspension is not affecting the electrostatic repulsion between surfaces. Pedersen and Bergstrom[8] postulated that repeated contacts between zirconia surfaces with poly(acrylic acid) dispersants led to adhesive forces until polymer was "packed" between the contact zones to form a repulsive barrier. The higher required concentration of polyelectrolyte for this powder may result from the need for dense adsorbed layers to resist aggregation from multiple particle collision events.

For the steric Hypermer KD-1 surfactant, the optimum dispersant concentration was determined by measurements of viscosity at 20 vol %. A concentration of 4 wt % surfactant was found to give the lowest viscosity values. This is comparable with the poly(methacrylic acid) concentration required for dispersion. Because the molecular weight of the dispersant is proprietary, it is likely that the higher mass ratio relates to a higher molecular weight for the dispersant molecule and potentially a larger interparticle separation distance.

Rheology data for the suspensions with each dispersant were measured for a number of volume fractions. In Figure 6, only the profiles near 30 vol % are shown to indicate the difference in behavior between each dispersant type under similar conditions in solids loading between the surfactants. Because the Darvan C surfactant had greater performance than the others, the profile at 37 vol % is also presented. The shear rate measurements show that the behavior of the suspensions looks nearly linear on a log-log plot. The slope in these plots is a function of volume fraction, and at lower solids loading the slope of the log-log plots for the Darvan C and Hypermer KD-1 dispersed systems is very low and exhibits only mild shear thinning behavior. For sodium citrate and native powder, the rheological response is highly shear thinning at all solid loadings, which suggests that these systems are flocculated. For dispersed systems, shear thinning is only pronounced at the highest solid contents measured.

The viscosity values at 400 s^{-1} were used for plotting the behavior of the suspensions against solids loading in Figure 7. Clearly, the polyelectrolyte dispersant (Darvan C) demonstrates the greatest capability for forming high solids content suspensions. The near linear responses of the native and sodium citrate suspensions plotted in a semi-log fashion are very similar to the behavior of salt flocculated systems.[33] Further study of rheological properties is necessary to determine whether the suspension behaves according to theories of gelled systems, which are based on percolation theory. The sodium citrate suspension exhibits lower viscosities than the native powder, and the steric length of the adsorbate has been predicted to be approximately 0.5–1.0 nm.[34, 35] Because the van der Waals interaction is hyperbolic at very short (<5 nm) ranges, the adsorption of the citrate ion can be expected to create this reduction in viscosity. Luther et al.[35] observed a similar reduction in the viscoelastic properties of flocculated suspensions at the native isoelectric point and at the isoelectric point in the presence of citrate.

For the two dispersed systems, shear thinning is observed and a constant viscosity is approached at high shear rates. Plots of high shear viscosity versus volume fraction are typically fit with a modified Krieger–Doughtery relationship:[8]

$$\eta_r = \left(1 - \frac{\phi}{\phi_{max}}\right)^{-n\phi_{max}} \quad (3)$$

Here, η_r is the relative viscosity, ϕ_{max} is the maximum solids loading, and n is factor describing the increase in viscosity. The native and citric acid systems could not be fit using this equation, but both the Hypermer KD-1 and Darvan C dispersed suspensions did generate realistic fitting parameters as given in Table II. The rheology data predict that maximum packing will be achieved for the KD-1 system at 35 vol % and at 40 vol % for the Darvan C system.

From Figure 7, the slope of the relative viscosity data points away from the maximum packing boundary is very similar between the two dispersed systems. This indicates

RESEARCH ARTICLE

that both systems are stable until the volume fraction of powder approaches the packing limit. The difference in maximum packing attainable for each system can be attributed to the volume of the surfactant. Dietrich et al.[10] used linear polyelectrolytes and predicted a monolayer thickness of 3–5 nm. Under high salt conditions, the electrostatic interaction will be screened, and the dispersant will present a largely steric interaction. Our calculation for a 50-nm particle correlates well with this result, as the expected true packing fraction for a 5-nm barrier is ~37 vol %. The steric length of the Hypermer KD-1 surfactant is taken to be that of a typical commercial surfactant near 5–10 nm. The lower maximum volume fraction predicted from the rheology data is expected based on these assumptions. A more defined study is needed to characterize these interparticle separations.

5. CONCLUSIONS

The nanosized alumina powder showed properties similar to those of conventional alumina materials for phase stability and isoelectric point. The magnitude of the zeta potential generated by the native powder surface and in the presence of aqueous surfactants is lower than that typically seen for conventional powders but is in agreement with that of nanopowders. The enhanced solubility of the nanopowder leads to some phase transformation and may be responsible for lower zeta potential values through dissolution and complexation with the surface groups.

In the dispersed state at low solids loading, particle association was modeled from acoustic data and suggested that particles associate at short range but do not agglomerate. Once agglomeration was initiated by lowering of the surface potential, agglomerate size was seen to increase, and the particle association phenomena disappeared. The phenomenon is theorized to result from the particle size distribution and crystallographic differences that generate variations in zeta potential and van der Waals interactions.

The dispersion of these alumina powders can be achieved using conventional polymeric surfactants but not with the small molecule surfactant studied here. Based on the sub-100 nm mean particle size, the maximum attainable volume fraction will be limited by the volume of surfactant, and a successful route to forming materials or composites from nanosize powders will be needed to minimize the volume of the dispersion mechanism. The optimal approach must be resistant to high salt concentrations, adsorb strongly to the powder, and have a low steric profile. Additional studies of the rheological properties of sub-100 nm powders is necessary to understand and optimize high solids loading dispersion.

References and Notes

1. E. Laarz, M. Carlsson, B. Vivien, M. Johnsson, M. Nygren, and L. Bergstrom, *J. Eur. Ceram. Soc.* 21, 1027 (**2001**).
2. R. B. Bagwell and G. L. Messing, *J. Am. Ceram. Soc.* 82, 825 (**1999**).
3. R. B. Bagwell, G. L. Messing, and P. R. Howell, *J. Mater. Sci.* 36, 1833 (**2001**).
4. C. S. Nordahl and G. L. Messing, *J. Am. Ceram. Soc.* 79, 3149 (**1996**).
5. N. S. Bell, J. Sindel, F. Aldinger, and W. M. Sigmund, *J. Coll. Interface Sci.* 254, 296 (**2002**).
6. S. Biggs and T. W. Healy, *J. Chem. Soc. Faraday Trans.* 90, 3415 (**1994**).
7. H. G. Pedersen and L. Bergstrom, *J. Am. Ceram. Soc.* 82, 1137 (**1999**).
8. L. Bergstrom, E. Blomberg, and H. G. Pedersen, *Key Eng. Mater.* 159–160, 119 (**1999**).
9. J. L. Deiss, P. Anizan, S. El Hadigui, and C. Wecker, *Coll. Surf. A* 106, 59 (**1996**).
10. A. Dietrich, A. Neubrand, and Y. Hirata, *J. Am. Ceram. Soc.* 85, 2719 (**2002**).
11. T. Hinklin, B. Toury, C. Gervais, F. Babonneau, J. J. Gislason, R. W. Morton, and R. M. Laine, submitted for publication.
12. A. S. Dukhin and P. J. Goetz, in *Handbook on Ultrasonic and Dielectric Characterization Techniques for Suspended Particulates*, edited by V. A. Hackley and J. Texter, The American Ceramic Society, Westerville, OH (**1998**), p. 77.
13. A. S. Dukhin, P. J. Goetz, and S. Takeda, www.dispersion.com.
14. R. Jenkins and R. L. Snyder, *Introduction to X-Ray Powder Diffractometry*, Wiley, New York (**1996**), p. 374.
15. W. H. Gitzen, *Alumina as a Ceramic Material*, The American Ceramic Society, Westerville, OH (**1970**), p. 22.
16. S. Kwon and G. L. Messing, *Nanostruct. Mater.* 8, 399 (**1997**).
17. E. Laiti, P. Persson, and L.-O. Ohman, *Langmuir* 14, 825 (**1998**).
18. J. Isrealachvili, *Intermolecular and Surface Forces*, Academic Press, New York (**1992**).
19. L. Bergstrom, *J. Chem. Soc. Faraday Trans.* 88, 3201 (**1992**).
20. W. N. Rowlands, R. W. O'Brien, R. J. Hunter, and V. Patrick, *J. Coll. Interface Sci.* 188, 325 (**1997**).
21. N. Kallay and S. Zalac, *J. Coll. Interface Sci.* 253, 70 (**2002**).
22. D. Velegol, S. Catana, J. L. Anderson, and S. Garoff, *Phys. Rev. Lett.* 83, 1243 (**1999**).
23. R. Kummert and W. Stumm, *J. Coll. Interface Sci.* 75, 373 (**1980**).
24. Y. Liu, L Gao, and J. Guo, *Coll. Surf. A* 193, 187 (**2001**).
25. P. C. Hidber and L. J. Gauckler, *J. Am. Ceram. Soc.* 79, 1857 (**1996**).
26. P. C. Hidber, T. J. Graule and L. J. Gauckler, *J. Eur. Ceram. Soc.* 17, 239 (**1997**).
27. Y. Mao and B. M. Fung, *J. Coll. Interface Sci.* 191, 216 (**1997**).
28. K. Gotoh, T. Inoue, J. Inada, and M. Tagawa, *J. Dispersion Sci. Techno.* 19, 475 (**1998**).
29. J. Widegren and L. Bergstrom, *J. Am. Ceram. Soc.* 85, 523 (**2002**).
30. J. Cersarano III, I. A. Aksay, and A. Bleier, *J. Am. Ceram. Soc.* 71, 250 (**1988**).
31. J. Cesarano III and I. A. Aksay, *J. Am. Ceram. Soc.* 71, 1062 (**1988**).
32. A. Zupancic, R. Lapasin, and A. Kristoffersson, *J. Eur. Ceram. Soc.* 18, 467 (**1998**).
33. J. A. Yanez, T. Shikata, F. F. Lange, and D. S. Pearson, *J. Am. Ceram. Soc.* 79, 2917 (**1996**).
34. S. Biggs, P. J. Scales, Y.-K. Leong, and T. W. Healy, *J. Chem. Soc. Faraday Trans.* 91, 2921 (**1995**).
35. E. P. Luther, J. A. Yanez, G. V. Franks, F. F. Lange, and D. S. Pearson, *J. Am. Ceram. Soc.* 78, 1495 (**1995**).

Received: 3 March 2003. Revised/Accepted: 14 July 2003.

RESEARCH ARTICLE